Eur Biophys J (2000) 29: 104–112 

ARTICLE

**David L. Turner · Lorraine Brennan · Ana C. Messias**
**Miguel L. Teodoro · António V. Xavier**

# Correlation of empirical magnetic susceptibility tensors and structure in low-spin haem proteins

Received: 3 September 1999 / Accepted: 10 December 1999

**Abstract** Experimental magnetic susceptibility tensors are reported for eight haems *c* with bis-His coordination. These data, obtained by fitting the dipolar shifts of backbone protons in the tetrahaem cytochromes $c_3$ from *Desulfovibrio vulgaris* and *D. gigas*, are analysed together with published values for other haem proteins. The *x* and *y* axes are found to rotate in the opposite sense to the axial ligands and are also counter-rotated with respect to the frontier molecular orbitals of the haem. The magnetic *z*-axis is close to the normal to the haem plane in each case. The magnitudes of the magnetic anisotropies are used to derive crystal field parameters and the rhombic splitting, *V*, is correlated with the dihedral angle between the axial ligands. Hence, it is apparent that the axial ligands are the dominant factor in determining the variation in magnetic properties between haems, and it is confirmed that "high $g_{max}$" EPR signals are a reliable indicator of near-perpendicular ligands. These results are in full agreement with the analysis of non-Curie effects and electronic structure in the His-Met coordinated cytochromes *c* and $c_{551}$. Collectively, they show that the orientations of axial ligands to the haem may be estimated from single-crystal EPR data, from $^{13}$C NMR shifts of the haem substituents, or from NMR dipolar shifts of the polypeptide.

## Introduction

The essential theory of the electronic and magnetic properties of low-spin Fe(III) complexes with perturbed cubic symmetry is well established (Griffith 1957; Oosterhuis and Lang 1969; Horrocks and Greenberg 1973), but its application to haem proteins has been restricted by uncertainty about the effects of the reduced symmetry that results from distorted porphyrins, asymmetric substitution, and the surrounding protein. Obviously, the geometry of the axial ligands is a dominant factor in complexes of symmetrically substituted porphyrins, but the literature relating to native proteins is equivocal (Walker 1999). The structure of the two frontier molecular orbitals (MOs) of the porphyrin can be probed directly using $^{13}$C NMR of the haem substituents and studies have shown that it is dominated by the geometry of the axial ligands (Turner et al. 1995; Louro et al. 1998). That work established the link between the ligands and the perturbation in the plane of the haem; we now seek to test the relationship between the magnetic susceptibility tensor and the ligand geometry. Understanding the magnetic properties of the haem is more complicated because the three iron orbitals of $t_{2g}$ symmetry ($d_{xy}$, $d_{xz}$, $d_{yz}$) must be considered. The experiments are also more difficult: ideally, EPR studies require single crystals, and NMR studies of dipolar shifts in solution require extensive assignment of signals in paramagnetic and diamagnetic forms of the protein (Keller and Wüthrich 1972). In either case, a structure is necessary to define the orientation of the magnetic susceptibility tensor with respect to the protein.

Apart from the nuclei of the haem and its ligands, which also experience Fermi contact shifts, paramagnetic shifts in haem proteins are well described by the approximation of metal centred dipolar shifts, in which it is assumed that the unpaired electron is localised on the metal ion (Bertini and Luchinat 1986). There is a complication insofar as any redox-state-related change in the structure of the protein may alter the diamagnetic contribution to the chemical shifts and, hence, the shift differences observed between paramagnetic and diamagnetic forms are only an approximate measure of the dipolar shifts of the nuclei. In fact, anomalous redox-state-related shifts have been used to locate regions of

D.L. Turner (✉)
Department of Chemistry, University of Southampton,
Southampton SO17 1BJ, UK
e-mail: dlt@soton.ac.uk

L. Brennan · A.C. Messias · M.L. Teodoro · A.V. Xavier
Instituto de Tecnologia Química e Biológica,
Universidade Nova de Lisboa, Oeiras, Portugal

the structure of mitochondrial cytochrome *c* that change when the protein is oxidised (Williams et al. 1985; Feng et al. 1990; Turner and Williams 1993).

If the structures of the paramagnetic and diamagnetic forms of a protein in solution are virtually identical and the coordinates are known, the magnetic susceptibility tensor can be fitted accurately to a set of measured $^1$H dipolar shifts. Conversely, atomic coordinates may be refined with respect to dipolar shifts if the magnetic susceptibility tensor is known (Barry et al. 1971; Gochin and Roder 1995; Banci et al. 1996, 1997, 1998; Turner et al. 1998). However, it is important to recognise the limitations imposed by the approximate nature of the measured shifts.

Despite the number of crystal structures and NMR studies reported for haem proteins, magnetic susceptibility tensors are available in surprisingly few cases. Recently, Shokhirev and Walker (1998) presented an analysis of atomic d-orbitals in a distorted cubic field and used published data to test the expectation that the rhombic perturbation and the magnetic axes should rotate in opposite senses in the plane of a low-spin haem (Oosterhuis and Lang 1969), but they found the relationship between ligand orientation and the axes to be inconclusive. We now present data for a further eight haems *c* with bis-histidine coordination and re-evaluate the evidence for counter-rotation of the perturbation and magnetic axes and their relationship with the geometry of the axial ligands to the iron. The experimental shifts are taken from the oxidised and reduced forms of the tetrahaem cytochromes $c_3$ from *Desulfovibrio vulgaris* (Hildenborough) and *D. gigas*. Crystal structures are available for the oxidised forms of both proteins (Matias et al. 1996; Simões et al. 1998), and the analysis is restricted to protons of the backbone to minimise the possible influence of redox state related changes in structure. Furthermore, the electronic structure of each haem has been determined previously from $^{13}$C NMR data (Louro et al. 1998).

The empirical magnetic susceptibility tensors presented here nearly double the number of haems for which comprehensive data are available; unfortunately, the conventions used in some articles are ambiguous. Collectively, the data confirm that the magnetic *z*-axis is found within a few degrees of the normal to the haem plane, and that the magnetic *y*-axis rotates in the plane of the haem in the opposite sense to the axial ligand orientations. Independently, the magnetic axes show a good correlation with counter-rotation with respect to the rhombic perturbations that define the form of the haem MOs which have been characterised by $^{13}$C NMR measurements. The axial and rhombic anisotropies of the magnetic susceptibility tensors are analysed quantitatively, and the magnitude of the rhombic perturbation clearly correlates with the dihedral angle between the imidazole planes of the axial ligands. This confirms that the geometry of the axial ligands is the dominant factor in systems with the "large $g_{max}$" or "HALS" type of EPR spectrum (Gadsby and Thomson 1986; Walker et al. 1986) in proteins as well as in model complexes.

This work provides conclusive experimental evidence for the counter-rotation of magnetic axes with respect to the axial ligands in low-spin bis-histidinyl haem proteins and, therefore, the general utility of the theory of the non-Curie temperature dependence of their NMR spectra (Shokhirev and Walker 1995; Turner 1995). It also shows that $^{13}$C NMR assignment of haem resonances provides reliable data for deducing axial ligand orientations. This method is more straightforward than EPR or measuring dipolar shifts by NMR and requires minimal prior information about the protein structure.

## Materials and methods

### Experimental measurements

Cytochromes $c_3$ from *D. gigas* (c3Dg) and *D. vulgaris* (c3Dv) were purified as described previously (LeGall et al. 1971). The c3Dg sample was prepared by dissolving the lyophilised protein in 90% $H_2O$/10% $D_2O$ to a concentration of approximately 3.2 mM, and c3Dv was prepared at 2.5 mM in 92% $H_2O$/8% $D_2O$. The pH was adjusted with HCl or NaOH. The uncorrected pH readings were 5.1 and 7.1 for the solutions of oxidised c3Dg and c3Dv, respectively. The c3Dg sample was reduced by reaction with gaseous $H_2$ in the presence of catalytic amounts of the enzyme hydrogenase from *D. gigas* and the pH adjusted to 7.3.

The NMR experiments were carried out using a Bruker DRX500 spectrometer. For oxidised c3Dg, NOESY (Kumar et al. 1980) spectra (25 ms and 80 ms mixing time) were acquired with a spectral width of 22 ppm. The 80 ms NOESY spectrum was recorded with presaturation of the water signal by a composite 180° pulse followed by a SCUBA sequence to facilitate recovery of potentially saturated alpha protons (Brown et al. 1988). The 25 ms NOESY spectrum was recorded using a standard pulse sequence with presaturation of the water signal during the relaxation delay. TOCSY spectra were acquired with mixing times of 25 ms and 75 ms using a clean TOCSY pulse sequence (Bearden et al. 1988; Griesinger et al. 1988). COSY spectra were also acquired. A similar set of spectra was recorded for the oxidised form of c3Dv, and a set of spectra similar to that reported previously for reduced c3Dv (Messias et al. 1998) was recorded for reduced c3Dg.

The spectra were displayed and annotated using the computer program XEASY (Bartels et al. 1995). The complete set of assignments for reduced c3Dv has been published (Messias et al. 1998), and specific $^1$H assignments of the haem protons and several amino acids are available for the other spectra (Piçarra-Pereira et al. 1993; Salgueiro et al. 1997; Louro et al. 1998). The chemical shifts of the remaining backbone protons were obtained by identifying NOESY cross peaks to these

protons and using standard methods for sequential assignment (Wüthrich 1986). The dipolar shift of each proton is approximated by the simple difference of the shift in the oxidised and reduced samples.

### Data analysis

The shift of a nucleus generated by dipolar interaction with a rapidly relaxing electron with an anisotropic ***g***-tensor can be expressed in terms of the spherical polar coordinates $(r,\theta,\phi)$ of the nucleus with respect to the principal axis system of the magnetic susceptibility tensor and the axial and equatorial anisotropies, $\Delta\chi_{ax}$ and $\Delta\chi_{eq}$ (Bertini and Luchinat 1986):

$$\delta_{pc} = \frac{1}{12\pi r^3}\left[\Delta\chi_{ax}(3\cos^2\theta - 1) + \frac{3}{2}\Delta\chi_{eq}\sin^2\theta\ \cos 2\phi\right] \quad (1)$$

It is assumed that the electron is localised on the metal ion and a molecular axis system is defined with respect to the macrocycle and pyrrole nitrogens of the haem. The origin is placed at the centre of gravity, with the *z*-axis normal to the best plane through the haem and the *y*-axis along the vector N2-N4 (Williams et al. 1985; Turner et al. 1998). Given a set of atomic coordinates, the dipolar shift of any atom is defined by two anisotropies and three Euler angles that relate the magnetic axes to the molecular system. For the tetrahaem cytochromes, the observed shifts are the sum of contributions from the four haems and, therefore, a total of 20 parameters are required for each protein. Proton coordinates were calculated from the crystal structures 1wad (Simões et al. 1998) and 2cth (Matias et al. 1996) and the parameters of the magnetic susceptibility tensors were fitted iteratively using the Marquardt method, with weighting according to the local gradient in the dipolar field (Turner and Williams 1993).

The crystal field parameters $\Delta$ and $V$ were used to calculate and fit the magnetic anisotropies through diagonalisation of the Hamiltonian in the basis set of six $t_{2g}$ spin-wavefunctions (Oosterhuis and Lang 1969; Turner 1993). The full set of values for $\Delta\chi_{ax}$ and $\Delta\chi_{eq}$ was fitted with the assumption that all of the haems have identical values of $\Delta$ and of the spin-orbit coupling constant, $\lambda$.

## Results and discussion

The difference between the chemical shift of a nucleus in the paramagnetic oxidised protein and its shift in the reduced diamagnetic form comprises a number of terms:

$$\delta_{ox} - \delta_{red} = \delta_{mc} + \delta_{lc} + \delta_{Fc} + \Delta\delta_{dia} \quad (2)$$

Among these, the Fermi contact contribution, $\delta_{Fc}$, is significant only for nuclei of the haem and its ligands, which are excluded from this analysis. The ligand-centred dipolar shift, $\delta_{lc}$, might be significant for sidechains in van der Waals contact with the porphyrins or the imidazole ligands but should be small for the more distant backbone protons. A change in the diamagnetic contribution to shifts in the two forms, $\Delta\delta_{dia}$, may arise from redox-state-related changes in conformation. Comparison of the structure of reduced cytochrome c3Dv in solution and in the crystal structure, which is of the oxidised form, showed that the differences involved mainly localized sidechain reorientations (Messias et al. 1998); hence this term is likely to be small for backbone protons. The remaining term, $\delta_{mc}$, represents the metal-centred dipolar contribution that arises from the coupling between the nucleus and unpaired spin density localised on the metal ion, which is described by Eq. (1). This equation should, therefore, provide an accurate description of the redox-state-related shift differences that are listed in Table 1. Glycine $\alpha CH_2$ protons are excluded because the shift differences are ambiguous in the absence of stereospecific assignments for both oxidation states.

The coordinates of the nuclei with respect to the metal centres are essential to fitting the parameters of the magnetic susceptibility tensors, and these were obtained from crystal structures (Matias et al. 1996; Simões et al. 1998). The standard errors of the fits assume an uncertainty of $\pm 0.05$ ppm in each measured shift and $\pm 0.5$ Å in the position of each proton. A total of 151 shifts was used for the fitting of c3Dv, and 171 for c3Dg. The results are plotted in Fig. 1, and the optimised parameters are listed in Table 2, together with their standard errors. An additional appreciation of the effect of uncertainties in the atomic coordinates may be gained by comparing the results obtained using the structures of the two molecules (A and B) in the unit cell of c3Dv.

The quality of the fits is generally good, but significant deviations are found for residues 41–44 of c3Dv. These residues, close to haem I, are in a region which has been shown to undergo a redox-state-related change in conformation and to have significant values of $\Delta\delta_{dia}$ because of the change in ring current shifts induced by the haem (Messias et al. 1998). However, excluding these shifts had little effect on the fitted parameters, and they are included in the fits reported here.

The Euler angle $\beta$ represents the tilt in the *z*-axis away from the normal to the haem plane. In all cases the tilt is small, and the larger deviations are found for haems with near-parallel axial ligands. This would be expected if the tendency for the *z*-axis to lie in the imidazole plane in haems with an axial His ligand proves to be a general phenomenon (Brennan and Turner 1997). The angles $\alpha$ and $\gamma$ define the direction of the tilt and, therefore, have large errors when $\beta$ is small. However, the sum of $\alpha$ and $\gamma$ approximates the in-plane rotation of the *y*-axis of the magnetic susceptibility tensor when the *z*-axis is close to the haem normal, and this angle remains well defined. The values of $\alpha + \gamma$ are plotted against the orientation of the bisector of the normals to the imidazole planes of

**Table 1** Dipolar shifts (ppm) of protons in c3Dg at 306.4 K and cDv at 303.4 K

| Residue | c3Dg | | c3Dv | | Residue | c3Dg | | c3Dv | |
|---|---|---|---|---|---|---|---|---|---|
| | HN | HA | HN | HA | | HN | HA | HN | HA |
| 1 | | −1.08 | | −0.47 | 57 | 1.63 | 0.88 | | 1.04 |
| 2 | −1.46 | −1.50 | | −1.25 | 58 | 0.69 | 0.84 | | 0.50 |
| 3 | −1.45 | −4.82 | | −1.70 | 59 | 0.65 | 0.47 | 0.71 | 0.63 |
| 4 | | 0.96 | −1.54 | −5.92 | 60 | 0.53 | 1.25 | | 0.92 |
| 5 | 0.86 | 1.06 | | 0.81 | 61 | 0.51 | 0.50 | | 0.23 |
| 6 | 1.16 | 1.75 | 1.10 | 1.33 | 62 | 0.70 | 0.55 | 0.04 | 0.54 |
| 7 | 0.71 | | 1.51 | 1.91 | 63 | 0.48 | 0.83 | 1.22 | 3.77 |
| 8 | 0.43 | 0.19 | 0.79 | | 64 | 0.67 | 0.40 | 2.34 | |
| 9 | −0.13 | −0.60 | 0.41 | 0.19 | 65 | 0.23 | 0.92 | 2.63 | 3.47 |
| 10 | −1.25 | −1.21 | −0.01 | −0.54 | 66 | 1.22 | 3.26 | 2.30 | 3.78 |
| 11 | −0.83 | −0.70 | −1.22 | −1.18 | 67 | 2.14 | 1.97 | 2.73 | 2.36 |
| 12 | −1.00 | −0.30 | −0.68 | −0.51 | 68 | 2.28 | 2.97 | 2.84 | 0.53 |
| 13 | −0.41 | 0.04 | −1.02 | −0.18 | 69 | 2.12 | 4.08 | 2.09 | −1.47 |
| 14 | −0.01 | −0.20 | −0.61 | −0.07 | 70 | 2.56 | 2.46 | | |
| 15 | −0.18 | | 0.02 | 0.15 | 71 | 2.19 | 0.56 | 1.82 | 1.46 |
| 16 | | | 0.00 | 1.47 | 72 | 1.49 | −1.16 | | 0.31 |
| 17 | −0.15 | −0.03 | | −0.46 | 73 | | | | −0.21 |
| 18 | −0.05 | 0.03 | −1.19 | −0.11 | 74 | 1.80 | 1.23 | −0.24 | −0.37 |
| 19 | 0.02 | −0.03 | −0.58 | −0.70 | 75 | 0.75 | 0.35 | −0.72 | −0.34 |
| 20 | 0.42 | 1.05 | −0.46 | −1.11 | 76 | 0.14 | −0.02 | −0.42 | 0.11 |
| 21 | 0.99 | −0.36 | 1.22 | 2.09 | 77 | −0.13 | | −0.37 | −1.28 |
| 22 | −1.18 | −0.12 | | | 78 | −0.72 | | −0.70 | −3.39 |
| 23 | −0.80 | −0.72 | 2.99 | 2.15 | 79 | −0.41 | 0.04 | | |
| 24 | −0.37 | −1.00 | 2.42 | 1.39 | 80 | −0.15 | 0.22 | −0.07 | 2.12 |
| 25 | 0.82 | 2.01 | | | 81 | | −1.09 | 0.16 | |
| 26 | | | 2.40 | 1.51 | 82 | −1.39 | −2.61 | | |
| 28 | 2.24 | 1.33 | 0.71 | −0.18 | 84 | −0.16 | 1.69 | 1.26 | 0.89 |
| 33 | −0.06 | | | | 89 | 0.26 | 0.09 | | 0.12 |
| 37 | | | 2.56 | 1.18 | 93 | 0.04 | 0.09 | 0.04 | −0.06 |
| 46 | 1.18 | 3.37 | | | 102 | 1.31 | 1.10 | 1.04 | 0.63 |
| 49 | | | 0.30 | 0.63 | 105 | 0.46 | 1.44 | | |
| 50 | 0.55 | 2.03 | 0.45 | | 106 | 1.22 | | | |
| 51 | 0.50 | 0.45 | | | 107 | 1.53 | 0.60 | 2.21 | 1.08 |
| 52 | 0.33 | 0.47 | | | 108 | 0.04 | −0.22 | | |
| 53 | 0.39 | | 2.62 | 1.56 | 109 | | | | |
| 54 | | | 2.07 | 1.03 | 110 | | | | |
| 55 | | | | 0.95 | 111 | | 1.08 | | |
| 56 | 2.32 | 1.34 | 0.78 | 0.50 | | | | | |

each haem, $\phi$, in Fig. 2. Results from the literature for other haems *b* and *c* with bis-His, His-Met, or His-CN coordination are collected in Table 3 and included in the plot. Angles quoted in the literature refer to a variety of molecular axis systems; these are all now referred to positive rotations going from pyrrole C to B, with zero along the bond from iron to the nitrogen of pyrrole C, as shown in Scheme 1. The values of $\alpha + \gamma$ are also plotted against the orientation of the rhombic perturbation, $\theta$, obtained from $^{13}$C NMR studies of the haem MOs in Fig. 2.

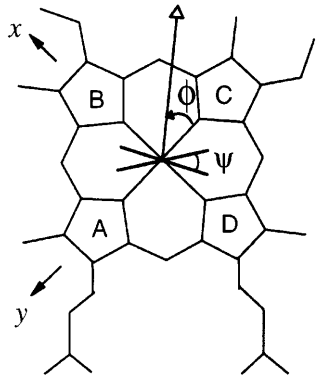


**Scheme 1**

The first conclusion that can be drawn is that the magnetic axes rotate in the opposite sense to the axial ligands or ligand (cyanide ligands are considered to be axially symmetric); the points that deviate most are those obtained with the smallest number of dipolar shifts or for proteins which have only approximate crystal structures, such as the peroxidases. Furthermore, when the angle between the imidazole normals (or between the normal and the Cγ-Sδ-Cε bisector in His-Met cytochromes) is large, the best correlation is with the average of the two; hence it is clear that both axial ligands contribute. Secondly, the correlation of $\alpha + \gamma$ with the negative value of $\theta$ from haem MOs is better than that with the ligand orientation, $\phi$. The values of $\theta$ are obtained from a different set of experimental data, $^{13}$C Fermi contact shifts as opposed to $^{1}$H dipolar shifts, and

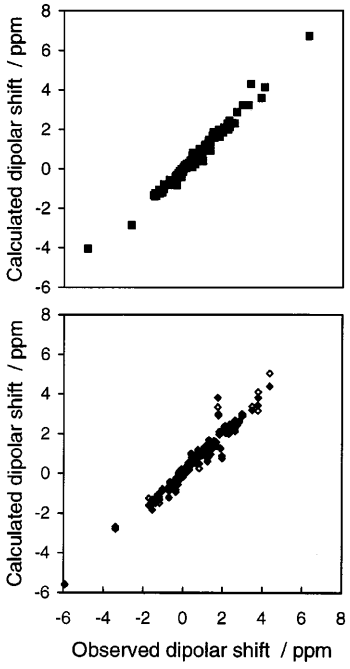


**Fig. 1** Observed and calculated dipolar shifts of backbone protons in c3Dg (*upper plot*) and c3Dv (*lower plot*). Separate fits for the two molecules in the unit cell of c3Dv are shown as *filled* and *empty symbols*

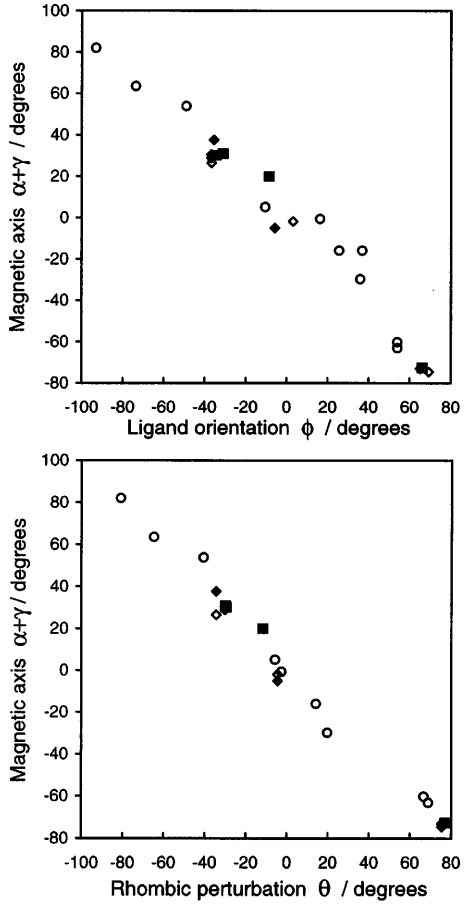


**Fig. 2** Orientations of magnetic axes in the haem plane plotted against the orientations of the axial ligands (*upper plot*) and of the MO perturbations (*lower plot*). Data for c3Dg (■) and c3Dv molecules A (◆) and B (◇) are listed in Tables 2 and 4, and *open circles* are from literature values listed in Table 3

the analysis involves two $\pi$ MOs as opposed to three iron atomic orbitals. This indicates that the approximations made in each case are rather good, and that both viewpoints reflect the properties of the covalently bonded iron with reasonable accuracy. The poorer correlation with angles taken from crystal structures is probably due to differences between structures in solution and in the crystal. This is an obvious problem in cases in which structures of homologous proteins were used, but it is a source of uncertainty in general. For example, the two molecules in the unit cell of lignin peroxidase have ligand orientations that differ by 11.2°, and those of haem II in c3Dv differ by 9.0°. It is also possible that the parameters of the magnetic suscepti-

**Table 2** Parameters of the empirical magnetic susceptibility tensors obtained by fitting proton dipolar shifts in the tetrahaem cytochromes c3Dg and c3Dv[a]

| Haem | $\alpha$ (deg) | | $\beta$ (deg) | | $\gamma$ (deg) | | $\alpha + \gamma$ (deg) | | $\Delta\chi_{ax} \times 10^{32}$ ($m^3$) | | $\Delta\chi_{eq} \times 10^{32}$ ($m^3$) | |
|---|---|---|---|---|---|---|---|---|---|---|---|---|
| c3Dg | | | | | | | | | | | | |
| I | 37.4 | (18.5) | −5.3 | (1.9) | −7.3 | (17.0) | 30.1 | (4.0) | 2.94 | (0.15) | −1.89 | (0.17) |
| II | 48.6 | (16.4) | 4.4 | (1.4) | −28.7 | (16.7) | 19.9 | (3.7) | 3.17 | (0.15) | −1.32 | (0.14) |
| III | −27.3 | (22.6) | −3.7 | (1.4) | −45.3 | (22.3) | −72.6 | (3.9) | 2.61 | (0.13) | −1.46 | (0.21) |
| IV | 18.5 | (6.8) | 11.1 | (1.3) | 12.3 | (7.0) | 30.8 | (2.9) | 3.05 | (0.14) | −1.45 | (0.13) |
| c3Dv (A) | | | | | | | | | | | | |
| I | 54.4 | (36.4) | 2.3 | (1.8) | −16.8 | (38.6) | 37.6 | (6.0) | 3.27 | (0.16) | −1.48 | (0.14) |
| II | 48.0 | (29.5) | 2.7 | (1.2) | −53.1 | (29.0) | −5.1 | (3.7) | 3.64 | (0.16) | −1.51 | (0.19) |
| III | −62.1 | (7.8) | −8.5 | (2.0) | −11.0 | (7.4) | −73.1 | (3.1) | 2.96 | (0.15) | −2.03 | (0.23) |
| IV | 6.9 | (12.4) | 7.2 | (1.9) | 22.0 | (12.5) | 28.8 | (3.2) | 3.13 | (0.16) | −1.76 | (0.13) |
| c3Dv (B) | | | | | | | | | | | | |
| I | −75.3 | (37.4) | −2.7 | (1.6) | 101.7 | (37.0) | 26.4 | (3.8) | 3.24 | (0.18) | −1.96 | (0.17) |
| II | 50.5 | (21.9) | 3.5 | (1.3) | −52.5 | (21.5) | −1.9 | (4.3) | 3.78 | (0.17) | −1.41 | (0.18) |
| III | −72.0 | (7.6) | −8.7 | (2.3) | −2.6 | (7.5) | −74.6 | (2.9) | 2.84 | (0.15) | −2.06 | (0.25) |
| IV | 2.3 | (12.5) | 7.1 | (1.8) | 28.2 | (12.6) | 30.5 | (3.0) | 3.24 | (0.16) | −1.90 | (0.13) |

[a] Proton coordinates were generated from the structures 1wad and 2cth (molecules A and B). Standard errors given in parentheses are based on 0.05 ppm uncertainty in dipolar shifts and 0.5 Å in coordinates

**Table 3** Orientation (degrees) in the haem plane of the magnetic *y*-axes, the axial His ligands, and the rhombic perturbation of the haem MOs in various proteins

| Protein | $\alpha + \gamma$[a] | $\phi$[b] | $\theta$[c] | Ref. |
|---|---|---|---|---|
| Horse cyt *c* | 5.1 | −10.5 | −5.7 | Turner (1995) |
| *Ps. a.* cyt $c_{551}$ | 63.5 | −73.6 | −64.7 | Turner (1995) |
| Rat cyt $b_5$ A | −60.2 | 54.1 | 66.7 | Banci et al. (1995) |
| Rat cyt $b_5$ B | −29.8 | 36.0 | 19.8 | Banci et al. (1995) |
| Bovine cyt $b_5$ | −63.1 | 54.1 | 68.9 | Pierattelli and Turner (1996) |
| Mb-CN | 82.0 | −93.0 | −80.9 | Banci et al. (1995); Nguyen et al. (1999) |
| HRP-CN | −0.6 | 16.3 | −2.6 | Pierattelli et al. (1996) |
| LiP-CN | −16.0 | 36.9, 25.7[d] | 14.2 | Pierattelli et al. (1996) |
| M80A cyt *c*-CN | 53.8 | −49.0[e] | −40.6[f] | Banci et al. 1996; Brennan and Turner (1997) |

[a] The in-plane rotation of the magnetic axes is approximated by the sum of the Euler angles, $\alpha$ and $\gamma$, when the *z*-axis lies close to the haem normal
[b] The ligand orientation is the bisector of the acute angle between imidazole normals for bis-His haems, that of the imidazole normal and the Met lone pair in His-Met haems, and the imidazole normal itself in His-CN complexes
[c] The value $\theta$ is obtained from the analysis of $^{13}$C Fermi contact shifts (Louro et al. 1998)
[d] Two molecules per unit cell
[e] The His orientation from horse cytochrome *c*
[f] Rhombic perturbation measured in wild-type cytochrome *c*-CN

bility tensors and MOs experience similar secondary effects from different axial ligands and from low-symmetry distortions other than those caused by the ligands.

The remaining parameters, the axial and equatorial anisotropy, $\Delta\chi_{ax}$ and $\Delta\chi_{eq}$, are commonly regarded as having only qualitative significance, with a low value of $\Delta\chi_{eq}$ being interpreted as evidence of near-perpendicular axial ligands. The values obtained for c3Dg and c3Dv (both molecules in the crystal) are plotted against the dihedral angle, $\psi$, between the axial imidazoles in Fig. 3. Although there is some indication of a dependence on $\psi$, with haems II from c3Dv and c3Dg having a higher axial anisotropy and a lower equatorial anisotropy, it is not obvious. The significance of the theoretical curves in Fig. 3 is explained below.

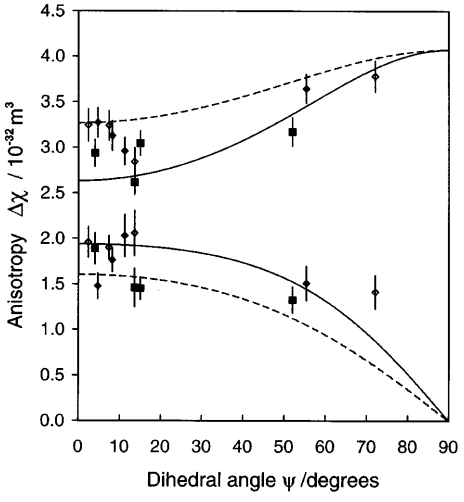


**Fig. 3** Fitted values of $\Delta\chi_{ax}$ and $\Delta\chi_{eq}$ (absolute values with error bars) in c3Dg (■) and c3Dv molecules A (◆) and B (◇) plotted as a function of the dihedral angle between the planes of the His ligands. The curves represent theoretical anisotropies for the upper (*solid line*) and lower (*dashed line*) limits of the rhombic splitting, *V*, at 305 K

The values of $\Delta\chi_{ax}$ and $\Delta\chi_{eq}$ reflect the separations of the three Kramers doublets, which are usually expressed in terms of the crystal field parameters, *V* and $\Delta$. There are large uncertainties associated with fitting two parameters to two others, therefore we assume that the axial splitting, $\Delta$, is the same for each of these bis-His haems and fit individual values of *V* and a single common value of $\Delta$. The value of $2.83\lambda$ obtained for $\Delta$ is well within the range 2.5–3.1 expected for bis-His ligated haems. Because the excited states are appreciably populated at room temperature, the absolute value of the spin-orbit coupling constant, $\lambda$, is significant. This was also treated as a common parameter and yielded the value 279 $cm^{-1}$, which lies between the value of 241 $cm^{-1}$ obtained from data for horse cytochrome *c* (Turner and Williams 1993) and the commonly assumed value of 340 $cm^{-1}$ (Williams et al. 1985). The analysis generates predicted *g*-values, listed in Table 4, and these are in reasonable agreement with experimental values obtained at liquid helium temperature. Figure 4 shows the plot of rhombic splittings, *V*, against the dihedral angles, $\psi$, obtained from the crystal structures.

Analysis of $^{13}$C data has shown that the energy separation of the frontier $\pi$ MOs of the haem is dominated by a cosine dependence on the dihedral angle $\psi$, with a secondary influence from the overall orientation of the axial ligands, $\phi$. The separation is approximately proportional to $(5 + \cos4\theta)\cos\psi$ (Louro et al. 1998). The theoretical curves in Figs. 3 and 4 represent the values of *V*, 20% each side of the central value, expected for axial ligands that have the resultant of their normals oriented either along an iron-pyrrole nitrogen bond ($\theta = \phi = 0$), or along an iron-*meso*-carbon vector ($\theta = \phi = \pi/4$). The central value was scaled to fit the values obtained for haems that have dihedral angles, $\psi$, less than 15°. In Fig. 3, curves are shown for calculated values of $\Delta\chi_{ax}$ and $\Delta\chi_{eq}$ with *V* taken to be proportional to $\cos\psi$ and scaled to the extreme values obtained for $\theta = 0$ and $\theta = \pi/4$. In principle, scaling the energy separation should not be necessary because the rhombic splitting

**Table 4** Fitted values of the rhombic splitting of the crystal field, $V$; calculated and observed values for $g_{max}$; His ligand orientations, $\phi$, and dihedral angles, $\psi$; and orientations of the molecular orbital perturbation, $\theta$, in the haems of c3Dg and c3Dv

| Haem | $V/\lambda$[a] | $g$ (calc) | $g$ (obs) | $\phi$ (deg)[b] | $\psi$ (deg)[b] | $\theta$ (deg)[c] |
|---|---|---|---|---|---|---|
| c3Dg | | | | | | |
| I | 1.76 | 2.96 | 2.96 | −34.6 | 4.0 | −29.6 |
| II | 1.27 | 3.18 | 3.05 | −8.6 | 52.0 | −11.7 |
| III | 2.01 | 2.86 | 2.94 | −23.9 | 13.6 | 77.1 |
| IV | 1.44 | 3.09 | 2.84 | −31.0 | 15.0 | −29.9 |
| c3Dv (A) | | | | | | |
| I | 1.31 | 3.16 | 2.96 | −35.5 | 4.7 | −34.4 |
| II | 1.10 | 3.27 | 3.14 | −5.8 | 55.4 | −4.5 |
| III | 1.79 | 2.95 | 2.80 | −24.9 | 11.2 | 75.4 |
| IV | 1.58 | 3.03 | 2.99 | −36.8 | 8.2 | −30.1 |
| c3Dv (B) | | | | | | |
| I | 1.59 | 3.02 | 2.96 | −36.7 | 2.4 | −34.4 |
| II | 0.99 | 3.33 | 3.14 | 3.2 | 72.1 | −4.5 |
| III | 1.90 | 2.90 | 2.80 | −20.7 | 13.6 | 75.4 |
| IV | 1.59 | 3.02 | 2.99 | −36.8 | 7.4 | −30.1 |

[a] Axial splitting $\Delta = 2.83\ \lambda$, $\lambda = 279\ cm^{-1}$, common to all haems
[b] From the crystal structures 1wad and 2cth (molecules A and B)
[c] Louro et al. (1998)

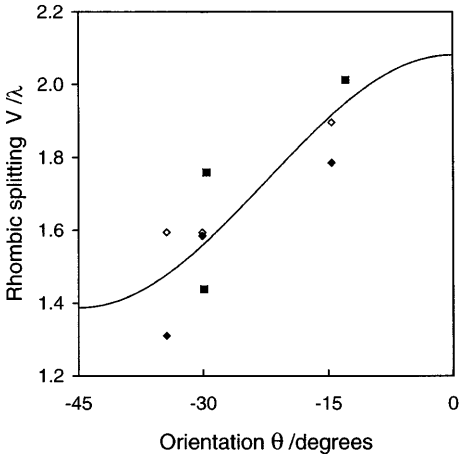


**Fig. 5** Plot of the rhombic splitting, $V$, as a function of the orientation of the MO perturbation in c3Dg (■) and c3Dv molecules A (◆) and B (◇). Only haems with a dihedral angle between the axial His ligands of less than 15° are included. The curve represents the function $5 + \cos(4\theta)$, scaled to the values in Fig. 4

also relates to the frontier $\pi$ MOs of the haem. However, delocalisation is neglected in fitting the magnetic susceptibility, and the apparent splitting depends on the MO coefficients (Louro et al. 1998). It is therefore satisfying that the splittings obtained by the two methods differ by less than 20%.

The lack of sensitivity of $\Delta\chi_{eq}$ to $\psi$ is immediately apparent from Fig. 3 and it is predicted to reach low values only when the axial ligands are very nearly perpendicular. The effect on the deduced crystal field parameter, $V$, is more clear in Figs. 4 and 5, although the uncertainties in the fitted anisotropies and, perhaps more importantly, possible variations in the axial splitting as a function of ligand geometry would make it difficult to obtain accurate values for the relative orientation of the ligands from the measurement of $^1$H dipolar shifts. In each case, it appears that the dihedral angle between the axial ligands of haem II in c3Dv in solution is closer to that of molecule A in the unit cell of the crystal.

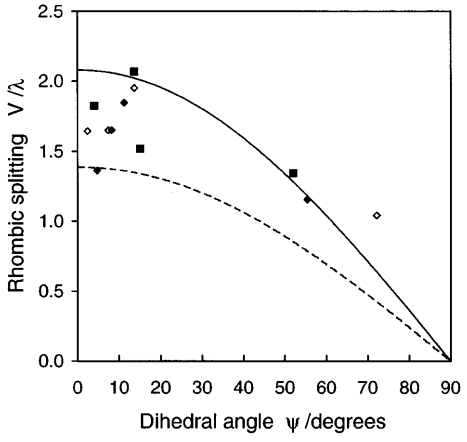


**Fig. 4** Fitted values of the rhombic splitting, $V$, as a function of the dihedral angle between the planes of the His ligands in c3Dg (■) and c3Dv molecules A (◆) and B (◇). The fits were obtained with simultaneous optimisation of the axial splitting ($\Delta = 2.83\ \lambda$) and the spin-orbit coupling constant ($\lambda = 279\ cm^{-1}$) common to all of the haems. The curves show the limits expected for ligands oriented along an iron-nitrogen bond (*solid line*) or aligned with *meso*-carbons (*dashed line*)

## Conclusion

The results presented here should leave no doubt that the axial ligands are the dominant factor in determining the rhombic distortion of the crystal field in low-spin haems *c*, that there is no significant difference between the influence of the proximal and distal ligands, and that counter-rotation of the ligands and the magnetic axes is indeed the norm. The uncertainty in the literature surveyed by Shokhirev and Walker (1998) is eliminated by considering the empirical tensors to be found in the recent literature together with the results presented here. The discrepancy of 12° found by Nguyen et al. (1999) between the value of $\alpha + \gamma$ and the His orientation in metmyoglobin cyanide cannot be regarded as inconsistent with counter-rotation in view of the quoted error of $\pm 5°$ for $\alpha + \gamma$ and the additional uncertainty in the His orientation taken from the crystal structure of carbonmonoxymyoglobin. In fact the Euler angles found in that work are remarkably similar to those obtained by Banci et al. (1995) from a smaller dataset and the agreement with $-\theta$, the value from MO analysis, is within 2°. However, the correlation is not expected to be as good for haems *b* as it is for haems *c* because of the influence of conjugation between the vinyl groups and

the haem macrocycle. The distortion caused by vinyl groups is relatively small (LaMar et al. 1978; Pierattelli and Turner 1996; Pierattelli et al. 1996), but Kolczak et al. (1999) found that replacing a vinyl group in cyanometmyoglobin with a formyl or an acyl group caused the hyperfine shifts of diametrically opposed methyl groups to differ by a factor of two or more. Clearly, the model of perturbed $D_4$ symmetry is not applicable to these modified haems.

Thus, although it appears that the dihedral angle between axial ligands can be deduced only qualitatively from magnetic anisotropies, it is clear that the average orientation of the two axial ligands may be obtained with useful accuracy from the principle of counter-rotation of the magnetic axes in low-spin haems *c*, and with only slightly less confidence in haems *b*.

The model required for the analysis of experimental proton dipolar shifts is significantly more complex than that used for the analysis of $^{13}C$ Fermi contact shifts in terms of haem MOs (Turner 1995; Louro et al. 1998), and the uncertainties in the fitted parameters are larger. Nonetheless, the two models are in broad agreement. The more precise results from $^{13}C$ NMR are likely to be most useful in providing constraints on the orientations of ligands, for which there may be no measurable nuclear Overhauser effects, for the purpose of determining structures of paramagnetic haem proteins. It is not necessary to know the protein structure a priori for the analysis of $^{13}C$ data and only the haem substituents need be assigned. However, $^{1}H$ dipolar shifts do contain valuable structural information. Using such data in structure calculations necessarily involves obtaining parameters for the magnetic susceptibility tensor, and it is clearly important to ensure that they are consistent with the ligand orientations in the published structures.

**Acknowledgements** The authors are grateful to Professor J. LeGall for kindly providing the protein samples. This work was supported by EC contract No. ERBFMRXCT980218 and by PRAXIS/PCNA/BIO/0074/96.

## References

Banci L, Pierattelli R, Turner DL (1995) Determination of haem electronic structure in cytochrome $b_5$ and metcyanomyoglobin. Eur J Biochem 232: 522–527

Banci L, Bertini I, Bren KL, Cremonini MA, Gray HB, Luchinat C, Turano P (1996) The use of paramagnetic shifts to refine solution structures of paramagnetic metalloproteins: Met80Ala cyanocytochrome *c* as an example. J Bioinorg Chem 1: 117–126

Banci L, Bertini I, Gray HB, Luchinat C, Reddig T, Rosato A, Turano P (1997) Solution structure of oxidised horse heart cytochrome *c*. Biochemistry 36: 9867–9877

Banci L, Bertini I, De La Rosa MG, Koulougliotis D, Navarro JA, Walter O (1998) Solution structure determination of oxidised cytochrome $c_6$ from green alga *Monoraphidium braunii*. Biochemistry 37: 4831–4843

Barry CD, North ACT, Glasel JA, Williams RJP, Xavier AV (1971) Quantitative determination of mononucleotide conformations in solution using lanthanide ion shift and broadening NMR probes. Nature 223: 236–245

Bartels C, Xia T, Billeter M, Güntert P, Wüthrich K (1995) The program XEASY for computer-supported NMR spectral-analysis of biological macromolecules. J Biomol NMR 6: 1–10

Bearden DW, Macura S, Brown LR (1988) Suppression of cross relaxation in TOCSY experiments on macromolecules. J Magn Reson 80: 534–538

Bertini I, Luchinat C (1986) NMR of paramagnetic molecules in biological systems. Benjamin/Cummings, Menlo Park, Calif

Brennan L, Turner DL (1997) Paramagnetic NMR shifts in cyanoferricytochrome *c*: investigation of thermal stability and deviations from Curie law behaviour. Biochim Biophys Acta 1342: 1–12

Brown SC, Weber PL, Mueller L (1988) Towards complete $^{1}H$ NMR spectra in proteins. J Magn Reson 77: 166–169

Feng Y, Roder H, Englander SW (1990) Redox-dependent structure change and hyperfine nuclear magnetic resonance shifts in cytochrome *c*. Biochemistry 29: 3494–3504

Gadsby PMA, Thomson AJ (1986) Low-temperature EPR and near-infrared MCD studies of highly anisotropic low-spin ferrihaem complexes. FEBS Lett 197: 253–257

Gochin M, Roder H (1995) Protein structure refinement based on paramagnetic NMR shifts; applications to wild-type and mutant forms of cytochrome *c*. Protein Science 4: 296–305

Griesinger C, Otting K, Wüthrich K, Ernst RR (1988) Clean TOCSY for $^{1}H$ spin system identification in macromolecules. J Am Chem Soc 110: 7870–7872

Griffith JS (1957) Theory of electron resonance in ferrihemoglobin azide. Nature 180: 30–31

Horrocks W, Greenberg ES (1973) Evaluation of dipolar nuclear magnetic resonance shifts in low-spin hemin systems: ferricytochrome *c* and metmyoglobin cyanide. Biochim Biophys Acta 322: 38–44

Keller RM, Wüthrich K (1972) The electronic *g*-tensor in cytochrome $b_5$: high resolution proton magnetic resonance studies. Biochim Biophys Acta 285: 326–336

Kolczak U, Hauksson JB, Davis NL, Pande U, deRopp JS, Langry KC, Smith KM, LaMar GN (1999) $^{1}H$ NMR investigation of the role of intrinsic heme versus protein-induced rhombic perturbations on the electronic structure of low-spin ferrihemoproteins: effect of heme substituents on heme orientation in myoglobin. J Am Chem Soc 121: 835–843

Kumar A, Wagner G, Ernst RR, Wüthrich K (1980) A two-dimensional nuclear Overhauser enhancement (2D NOE) experiment for the elucidation of complete proton-proton cross-relaxation networks in biological macromolecules. Biochem Biophys Res Commun 95: 1–6

LaMar GN, Viscio DB, Smith KM, Caughey WS, Smith ML (1978) NMR studies of low-spin ferric complexes of natural porphyrine derivatives. 1. Effect of peripheral substituents on the electronic asymmetry in biscyano complexes. J Am Chem Soc 100: 8085–8092

LeGall J, Bruschi HM, DerVartanian DV (1971) Electron paramagnetic resonance and light absorption studies on *c*-type cytochromes of the anaerobic sulfate reducer *Desulfovibrio*. Biochim Biophys Acta 234: 499–512

Louro RO, Correia IJ, Brennan L, Coutinho IB, Xavier AV and Turner DL (1998) Electronic structure of low-spin ferric porphyrins: $^{13}C$ NMR studies of the influence of axial ligand orientation. J Am Chem Soc 120: 13240–13247

Matias PM, Morais J, Coelho R, Carrondo MA, Wilson K, Dauter Z, Sieker L (1996) Cytochrome $c_3$ from *Desulfovibrio gigas*: crystal structure at 1.8Å resolution and evidence for a specific calcium-binding site. Protein Sci 5: 1342–1354

Messias AC, Kastrau DHW, Costa HS, LeGall J, Turner DL, Santos H, Xavier AV (1998) Solution structure of *Desulfovibrio vulgaris* (Hildenborough) ferrocytochrome $c_3$: structural basis for functional cooperativity. J Mol Biol 281: 719–739

Nguyen BD, Zhicheng X, Yeh DC, Vyas K, Deaguero H, LaMar GN (1999) Solution NMR determination of the anisotropy and orientation of the paramagnetic susceptibility tensor as a

function of temperature for metmyoglobin cyanide. J Am Chem Soc 121: 208–217

Oosterhuis WT, Lang G (1969) Mössbauer effect in $K_3Fe(CN)_6$. Phys Rev 178: 439–456

Piçarra-Pereira M, Turner DL, LeGall J, Xavier AV (1993) Structural studies on *Desulfovibrio gigas* cytochrome $c_3$ by two-dimensional NMR. Biochem J 294: 909–915

Pierattelli R, Turner DL (1996) Analysis of the paramagnetic shifts of haem carbon resonances in bovine ferricytochrome $b_5$. Eur Biophys J 24: 342–347

Pierattelli R, Banci L, Turner DL (1996) Indirect determination of magnetic susceptibility tensors in peroxidases: a novel approach to structure elucidation by NMR. J Biol Inorg Chem 1: 320–329

Salgueiro CA, Turner DL, Xavier AV (1997) Use of paramagnetic NMR probes for structural analysis in cytochrome $c_3$ from *Desulfovibrio vulgaris* Eur J Biochem 244: 721–734

Shokhirev NV, Walker FA (1995) Analysis of the temperature dependence of the $^1$H contact shifts in low-spin Fe(III) model hemes and heme proteins: explanation of "Curie" and "anti-Curie" behavior within the same molecule. J Phys Chem 99: 17795–17804

Shokhirev NV, Walker FA (1998) Co- and counterrotation of magnetic axes and axial ligands in low-spin ferriheme systems. J Am Chem Soc 120: 981–990

Simões P, Matias PM, Morais J, Wilson K, Dauter Z, Carrondo MA (1998) Refinement of the three-dimensional structures of cytochromes $c_3$ from *Desulfovibrio vulgaris* Hildenborough at 1.67 Å resolution and from *Desulfovibrio desulfuricans* ATCC 27774 at 1.6 Å resolution. Inorg Chim Acta 273: 213–224

Turner DL (1993) Evaluation of $^1$H and $^{13}$C Fermi contact shifts in horse cytochrome *c*: the origin of the anti-Curie effect. Eur J Biochem 211: 563–568

Turner DL (1995) Determination of haem electronic structure in His-Met cytochromes *c* by $^{13}$C-NMR. The effect of the axial ligands. Eur J Biochem 227: 829–837

Turner DL, Williams RJP (1993) $^1$H and $^{13}$C NMR investigation of redox-state dependent and temperature-dependent conformation changes in horse cytochrome *c*. Eur J Biochem 211: 555–562

Turner DL, Salgueiro CA, Schenkels P, LeGall J, Xavier AV (1995) Carbon-13 NMR studies of the influence of axial ligand orientation on haem electronic structure. Biochim Biophys Acta 1246: 24–28

Turner DL, Brennan L, Chamberlin SG, Louro RO, Xavier AV (1998) Determination of solution structures of paramagnetic proteins by NMR. Eur Biophys J 27: 367–375

Walker FA (1999) Magnetic spectroscopic (EPR, ESEEM, Mössbauer, MCD and NMR) studies of ferriheme centers and their corresponding heme proteins. Coord Chem Rev 186: 471–534

Walker FA, Huynh BH, Scheidt WR, Osvath SR (1986) Models of cytochrome *b*. Effect of axial ligand plane orientation on the EPR and Mössbauer spectra of low-spin ferrihemes. J Am Chem Soc 108: 5288–5297

Williams G, Clayden NJ, Moore GR, Williams RJP (1985) Comparison of the solution and crystal structures of mitochondrial cytochrome *c*, analysis of paramagnetic shifts in the nuclear magnetic resonance spectrum of ferricytochrome *c*. J Mol Biol 183: 447–460

Wüthrich K (1986) NMR of proteins and nucleic acids. Wiley, New York